BIOCHEMISTRY
including biophysical chemistry & molecular biology

Article

pubs.acs.org/biochemistry

Binding of TDP-43 to the 3′UTR of Its Cognate mRNA Enhances Its Solubility

Yulong Sun,[†] Pharhad E. Arslan,[‡] Amy Won,[§] Christopher M. Yip,[§] and Avi Chakrabartty*[,†,§]

[†]Department of Medical Biophysics, University of Toronto, Toronto, Ontario M5G 1L7, Canada

[‡]Tanz Centre for Research in Neurodegenerative Diseases, Faculty of Medicine, University of Toronto, Toronto, Ontario M5S 2J7, Canada

[§]Department of Biochemistry, University of Toronto, Toronto, Ontario M5S 1A8, Canada

Supporting Information

ABSTRACT: TAR DNA binding protein of 43 kDa (TDP-43) has been implicated in the pathogenesis of a broad range of neurodegenerative diseases termed TDP-43 proteinopathies, which encompass a spectrum of diseases ranging from amyotrophic lateral sclerosis to frontotemporal dementia. Pathologically misfolded and aggregated forms of TDP-43 are found in cytoplasmic inclusion bodies of affected neurons in these diseases. The mechanism by which TDP-43 misfolding causes disease is not well-understood. Current hypotheses postulate that the TDP-43 aggregation process plays a major role in pathogenesis. We amplify that hypothesis and suggest that binding of cognate ligands to TDP-43 can stabilize the native functional state of the protein and ameliorate aggregation. We expressed recombinant TDP-43 containing an N-terminal Venus yellow fluorescent protein tag in *Escherichia coli* and induced its aggregation by altering solvent salt concentrations and examined the extent to which various oligonucleotide molecules affect its aggregation *in vitro* using aggregation-induced turbidity assays. We show that vYFP-TDP-43 binding to its naturally occurring RNA target that comprises a sequence on the 3′UTR region of its mRNA improves its solubility, suggesting interplay among TDP-43 solubility, oligonucleotide binding, and TDP-43 autoregulation.

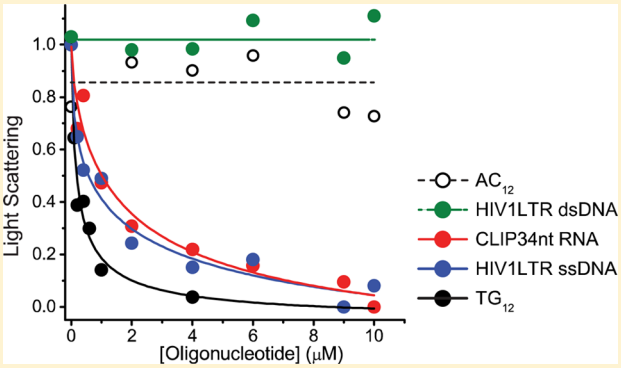

A common hallmark of neurodegenerative disease is the aggregation of misfolded proteins inside affected neurons.[1−3] Recent studies have identified TDP-43 as a major component of cytoplasmic aggregates within neurons of patients with amyotrophic lateral sclerosis (ALS),[4,5] and mutations in the TDP-43 gene (*TARDBP*) are known to be associated with familial ALS.[6] TDP-43 has since been implicated in a wide range of neurodegenerative diseases that run the gamut from ALS to frontotemporal lobar degeneration, which are now coined as TDP-43 proteinopathies.[7]

TDP-43 is a 414-amino acid nuclear protein composed of two highly conserved RNA recognition motifs (RRM1 and RRM2) and a C-terminal region (Figure S1A of the Supporting Information). These RRMs are involved in binding of RNA/DNA sequences enriched in UG or TG repeats.[8,9] Additionally, RRM2 mediates dimerization of the protein.[10] The C-terminal region is thought to mediate protein−protein interactions and contains yeast prion-like motifs implicated in disease pathology, and this region contains nearly all locations of disease-implicated mutations.[7,11−13]

Under pathological conditions, TDP-43 is found in cytosolic inclusion bodies, where it is hyperphosphorylated, ubiquitinated, and processed into 25 and 35 kDa C-terminal fragments.[4,5] Expression or introduction of these fragments in cell culture can recapitulate certain pathological features of TDP-43 proteinopathies by sequestration of wild-type TDP-43 from the nucleus and inducement of cell death through toxic gain of function.[14−16] One possible mechanism for TDP-43 misfolding involves the misfolding of the C-terminal domain into an aberrant structure that may act as a template for the recruitment of other, native TDP-43 molecules into this misfolded aggregate. The molecular mechanism of this conversion process is still a matter of debate. Cytoplasmic localization and recruitment into stress granule (SG) have been proposed as factors contributing to the initiation of TDP-43 aggregation.[17−20] Recent findings also suggest that RNA/DNA binding modulates TDP-43 solubility.[21,22]

TDP-43 conducts a variety of RNA processing functions in the cell, such as transcription, RNA regulation, micro-RNA processing, nucleo-cytoplasmic mRNA shuttling, and association with stress granules.[8,19,20,23,24] Because of its many functions, TDP-43 levels are tightly regulated. A proposed

Received: May 20, 2014
Revised: August 29, 2014
Published: August 29, 2014

   dx.doi.org/10.1021/bi500617x | *Biochemistry* 2014, 53, 5885−5894

mechanism of regulation is TDP-43 autoregulation by binding to the 3′UTR of its mRNA, leading to nonsense-mediated decay (NMD)-independent mRNA degradation and decreases in the level of TDP-43 production.[25−27]

To explore the possibility that nucleotide binding might regulate TDP-43 solubility, as well, we investigated the possibility that RNA/DNA binding prevents aggregation of TDP-43 and examined whether naturally occurring sequences, such as the autoregulatory binding region of the 3′UTR of TDP-43's mRNA, can modulate TDP-43 solubility. We hypothesized that binding of TDP-43 to its natural nucleotide ligands through its RRMs maintains TDP-43 in its soluble functional state, and the loss of this interaction in pathological situations may be an initiating factor for the aggregation of TDP-43 into inclusion bodies.

Using both natural ligands of TDP-43 and artificially constructed *de novo* sequences, we assess the effect of these compounds on TDP-43 aggregation and discuss the interplay between TDP-43 autoregulation and solubility.

EXPERIMENTAL PROCEDURES

Protein Expression and Purification. The pET-30 vector modified with a kanamycin resistance gene containing the recombinant wild-type vYFP-TDP-43 protein sequence or the F147L/F149L double mutant generated using the Q5 site-directed mutagenesis kit (New England Biolabs) (Figure S1B of the Supporting Information) was transformed into BL21-AI competent cells (Invitrogen), plated onto LB plates containing 35 μg/mL kanamycin (BioBasic), and incubated at 37 °C for 12 h. Colonies were inoculated into 2 mL of LB medium, incubated at 37 °C for 5 h, and diluted into 300 mL of LB medium. When the culture reached an absorbance of 0.4 at 600 nm, the temperature was reduced to 19 °C and the culture induced using 1 mM IPTG and 0.2% arabinose. Cells were harvested 6 h after induction by centrifugation at 3000 rpm (Sorvall SLA3000 rotor) for 20 min at 4 °C. The cell pellet was resuspended in 50 mL of lysis buffer [40 mM HEPES-KCl, 500 mM KCl, 20 mM imidazole, 20 mM $MgCl_2$, 2 mM βME, 10% glycerol, and complete EDTA-free protease inhibitor (Roche) (pH 7.4)].[28] Cells were lysed by sonication in 10 mL aliquots at 4 °C for 5 min (5 s pulse, 5 s stop) using a Vibracell sonicator (Sonics). The lysate was centrifuged for 30 min at 4 °C and 15000 rpm (Sorvall SS-34 rotor) to isolate the soluble protein fraction (supernatant). Purification of the His-tagged recombinant protein was achieved by Ni-NTA affinity chromatography using Ni-NTA beads (Sigma) at 4 °C. Ten milliliter of supernatant was applied to a 0.5 mL volume of Ni-NTA beads. The beads were washed twice with 1 mL of lysis buffer and eluted using modified lysis buffer containing 250 mM imidazole and no protease inhibitors to obtain purified protein.

Dynamic Light Scattering Measurements. Dynamic light scattering (DLS) measurements of the hydrodynamic radius (R_h) were taken at 20 °C with a DynaPro DLS instrument (Protein Solutions) using a 12 μL quartz cuvette. Samples were measured using an averaging time of 10 s. Ten or more consecutive measurements were used for regularization analysis using DYNAMICS software. Particle translational diffusion coefficients were calculated from decay curves of autocorrelation of light scattering data and converted to hydrodynamic radius (R_h) with the Stokes−Einstein equation. Histograms of mass versus R_h were calculated using Dynamics data analysis software.

Size Exclusion Chromatography. Purified vYFP-TPD-43 (40 μL, 20 mM) was injected into a Superdex 75 10/300 GL size exclusion column calibrated using YFP, BSA, RFP, and catalase at a flow rate of 0.5 mL/min. The protein signal was detected using a Waters 486 tunable absorbance detector at 515 nm with AUFS = 0.1.

Urea Denaturation. Purified protein samples (2 μM) were unfolded in 0−7.2 M urea and incubated for 30 min at room temperature. The Trp fluorescence and vYFP fluorescence of the samples were measured in a 1 cm cuvette using a Photon Technology International QM-1 fluorescence spectrophotometer using a λ_{ex} of 283 nm and a λ_{em} of 315−335 nm for Trp and a λ_{ex} of 515 nm and a λ_{em} of 528 nm for vYFP using a 2 nm bandpass. Integrated fluorescence was normalized and converted to percent folded for Trp fluorescence.

Circular Dichroism Spectroscopy. Purified protein was dialyzed against buffer containing 20 mM $MgCl_2$, 500 mM KCl, and 40 mM HEPES (pH 7.4) to remove imidazole for CD spectroscopy. Far-UV CD spectra were recorded with an Aviv CD spectrometer (model 62DS) at 25 °C. Spectra were obtained from 209 to 320 nm (1 mm path length, 1 nm step sizes, 1 nm bandwidth, and 16 s averaging time).

***In Vitro* Aggregation of vYFP-TDP-43.** Aggregation was induced by a 10-fold dilution of stock solutions of TDP-43 (20 μM) dissolved in 40 mM HEPES-KCl, 500 mM KCl, 250 mM imidazole, 20 mM $MgCl_2$, 2 mM βME, and 10% glycerol (pH 7.4) to a final concentration of 2 μM in 170 mM KCl, 36 mM HEPES, 25 mM imidazole, 18 mM $MgCl_2$, 1% glycerol, and 1.8 mM βME (pH 7.4), a method adapted from ref 28. For right angle light scattering measurements, samples were incubated for 4 h. For fluorescence microscopy and atomic force microscopy experiments, samples were incubated for 20 min.

Right Angle Light Scattering. Right angle light scattering (RALS) of aggregated samples was measured in a 1 cm quartz cuvette using a Photon Technology International QM-1 fluorescence spectrophotometer using an excitation wavelength of 400 nm and an emission wavelength of 400 nm with a 2 nm bandpass at room temperature. Emission was collected at 90° to the excitation source. Sample volumes of 200 μL were mixed before measurements. Twenty measurements were taken for each oligonucleotide concentration and averaged. Oligonucleotides were synthesized by Integrated DNA Technologies (Coralville, IA), desalted, and lyophilized, and their quality was assessed by mass spectrometry. Oligos were dissolved in DEPC-treated Milli-Q water immediately prior to being used. Inhibition curves were fit by nonlinear least-squares fitting to the equation

$$y = \frac{y_{max} - y_{min}}{1 + \left(\frac{x}{EC_{50}}\right)^n} + y_{min} \quad (1)$$

using OriginPro version 8.5, where y is the observed normalized scattering signal, x is the compound concentration, and n is the Hill coefficient.

Fluorescence Microscopy. Protein samples (9.25 μL) induced to aggregate in the presence or absence of oligonucleotides were inserted into a compartment constructed using Secure-Seal Imaging Spacers (Grace) and two no. 2 18 mm circular micro cover glass (VWR) for imaging. Fluorescence images were acquired on an Olympus IX70 (Olympus, Inc.) inverted microscope with a 40× TIRF objective (NA 1.45) (Olympus, Inc.), illuminated with a xenon light. Excitation light was reflected by a 485-555-

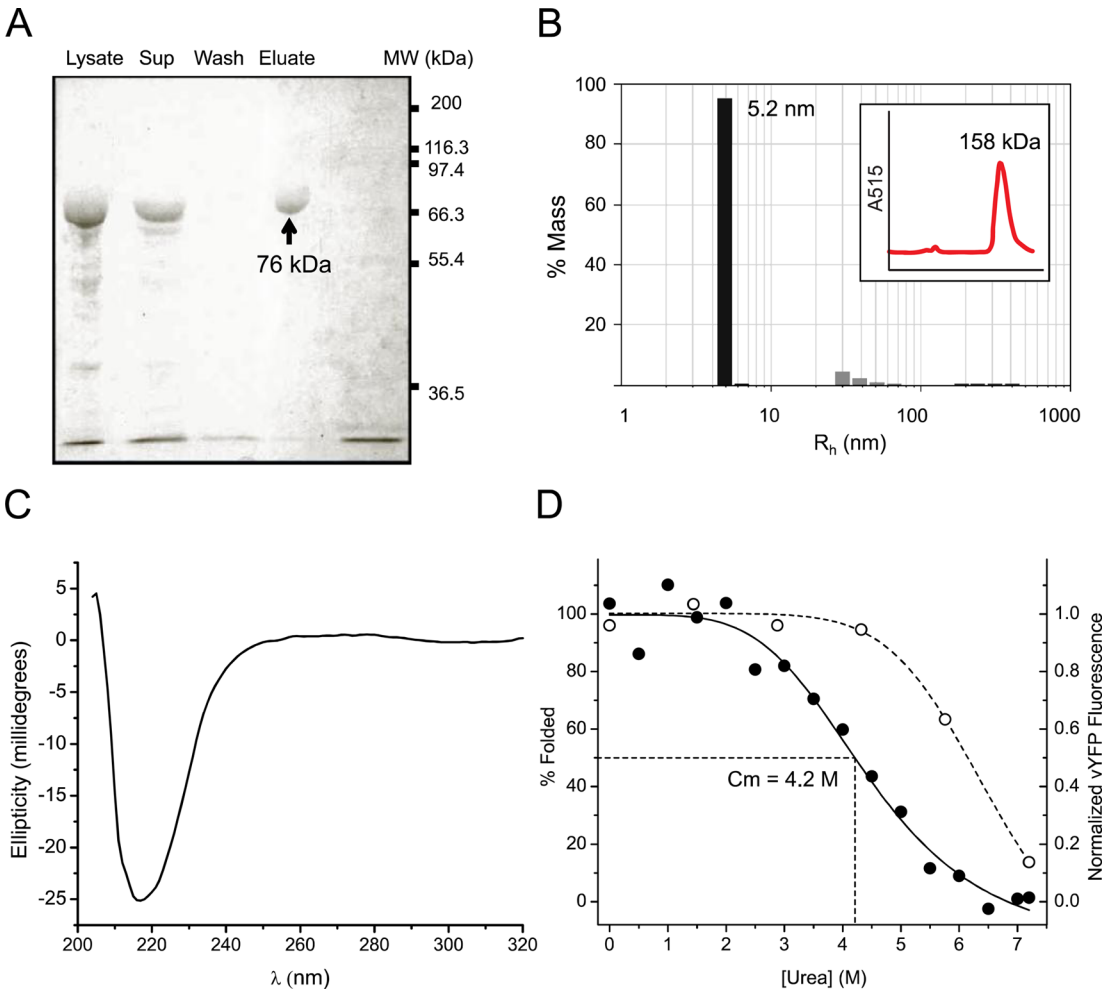

Figure 1. Characterization of vYFP-TDP-43 using various biochemical techniques. (A) SDS−PAGE of purified vYFP-TDP-43. Lanes containing the crude cell lysate after sonication (lysate), the soluble fraction of the cell lysate (sup), the fraction collected after washing with lysis buffer (wash), and final eluted fractions (eluate) are shown. Approximately 10 μg of each sample was applied to a 12% polyacrylamide gel for electrophoresis. The band corresponding to the size of vYFP-TDP-43 is indicated by the arrow. (B) Size distribution by mass of purified vYFP-TDP-43. A protein concentration of 20 μM was used. Measurements of R_h and MW were calculated using appropriate software (Experimental Procedures). The size exclusion chromatography peak of purified protein measured by vYFP absorbance and its estimated molecular mass is presented as an inset. (C) Circular dichroism spectrum of vYFP-TDP-43. Circular dichroism was measured at 25 °C with a 16 s averaging time. The signal for 8.8 μM vYFP-TDP-43 is shown with a characteristic β-signal. (D) Urea denaturation of vYFP-TDP-43. The integrated Trp fluorescence from 315 to 335 nm using excitation wavelength of 283 nm was measured for samples containing 2.1 μM vYFP-TDP-43 incubated with 0.0−7.2 M urea for 12 h. Trp fluorescence was normalized and converted to percent folded (●, left axis). vYFP fluorescence of the sample was measured by excitation at 515 nm and emission at 528 nm and normalized (○, right axis).

650TBDR dichroic, and emitted light was passed through a 515-600-730TBEM filter (Omega Optical, Inc.). Images were digitized with a cooled Evolution QEi CCD camera (Media Cybernetics, Inc.).

Atomic Force Microscopy. All atomic force microscopy (AFM) images were acquired using a glass tapping mode fluid cell with a Digital Instruments Nanoscope IIIA Multimode scanning probe microscope (Digital Instruments, Santa Barbara, CA). The AFM images were collected using Nanoscope version 5.12 and the J scanning head that has a maximal lateral scanning area of 116 μm × 116 μm. V-shaped silicon nitride probes (SNL-10 cantilever D, Bruker AFM Probes, Camarillo, CA) were irradiated under UV light for 30 min to remove organic contaminants. Protein samples (10 μL) induced to aggregate in the presence or absence of oligonucleotides were transferred onto freshly cleaved mica and sealed in the liquid cell. All images were captured as 512 × 512 scans at a tip scan rate between 0.7 and 1.2 Hz with a cantilever drive frequency of ∼8.5 kHz.

RESULTS

Recombinant vYFP-TDP-43 Is Natively Dimeric. TDP-43 is an intrinsically aggregation-prone protein.[28] To facilitate purification, enhance solubility, and act as a fluorescent probe, we attached an N-terminal Venus yellow fluorescent protein (vYFP) tag, which is a derivative of green fluorescent protein with mutations to increase its folding rate and brightness.[29,30] The construct was expressed in *Escherichia coli* using buffers adapted from previous studies.[28]

The quality of the expressed protein was assessed using a variety of assays. Sodium dodecyl sulfate−polyacrylamide gel electrophoresis (SDS−PAGE) of eluted samples confirms the presence of the single band at 76 kDa, corresponding to the expected size of recombinant vYFP-TDP-43 (Figure 1A). The

sample was also subjected to DLS and size exclusion chromatography (SEC) measurements to assess particle size under purification conditions. DLS results indicate a single species with a hydrodynamic radius of 4.86 nm, which constitutes 95% of the sample by mass (Figure 1B). Conversion of radius to molecular mass yields a mass of 136 kDa, consistent with dimer configuration, which was also observed in recent studies.[10] SEC measurments (inset) confirms the presence of a single peak at approximately 158 kDa. Circular dichroism spectroscopy on the eluted protein produced a spectrum indicative of β-structure with a characteristic β-structure signature at 218 nm (Figure 1C).[31] This was expected, as vYFP contains a β-barrel structure and contributes to this CD signal.[32] The absence of significant α-helix and random coil signals also indicate that TDP-43 is mostly β-structured, which agrees with recent crystallographic data of its RRM2 domain.[10] Urea denaturation of the sample monitored by Trp fluorescence and vYFP fluorescence shows cooperative unfolding of the entire construct with a denaturation midpoint of 4.2 M urea. The vYFP fluorescence is maintained at 100% at this urea concentration, suggesting that the observed unfolding curve is representative of the TDP-43 segment of the fusion protein (Figure 1D). The cooperative unfolding of the protein suggests that the TDP-43 segment of the recombinant protein is also folded. Collectively, these assays indicate that the protein produced was 95% pure, dimeric, and folded, and that the vYFP does not interfere with these intrinsic properties of TDP-43 under our experimental conditions.

TG_{12} Inhibits TDP-43 Aggregation at Substoichiometric Concentrations by Maintaining the Dimer Configuration. Recent studies have shown that poly-TG compounds can increase the solubility of refolded recombinant TDP-43 under aggregation conditions induced by temperature.[22] Here we investigated the concentration-dependent effect of aggregation inhibition by ssDNA consisting of 12 poly-TG repeats (TG_{12}) through turbidity measurements. Aggregation of vYFP-TDP-43 was reliably and reproducibly induced by ionic strength reduction using methods adapted from previously published works.[28] vYFP-TDP-43 (2 μM) was placed under aggregation conditions in the presence or absence of a 5-fold molar excess of TG_{12}, and the sizes of the particles were monitored using DLS and right angle light scattering (RALS). In the absence of nucleotides, incubation under aggregation conditions for 4 h at room temperature resulted in a majority of aggregates having hydrodynamic radii of 105.6 nm, with a significant secondary population with radii of up to 500−700 nm as measured by DLS. The estimated molecular mass of the average particle is approximately 18300 kDa (Figure 2A). In contrast, in the presence of 10 μM TG_{12} ssDNA, the average particle size had a hydrodynamic radius of 5.34 nm, corresponding to a molecular mass of 170 kDa, close to the theoretical size of the dimer (154 kDa) with two strands of TG_{12} (7.6 kDa) bound (Figure 2B). These findings were further validated by measurement of solution turbidity using RALS on samples incubated with or without a 5-fold molar excess of TG_{12} for 4 h. The level of scattering of the samples was significantly reduced by the presence of the TG_{12} compound (Figure 2C). When the soluble fractions of these samples were analyzed by DLS after centrifugation, untreated samples contained species corresponding to monomeric vYFP-TDP-43 (76 kDa) and soluble oligomers (~5000 kDa), while samples treated with TG_{12} remained dimeric (Figure 2D). These results indicate that TG_{12} is an effective inhibitor of

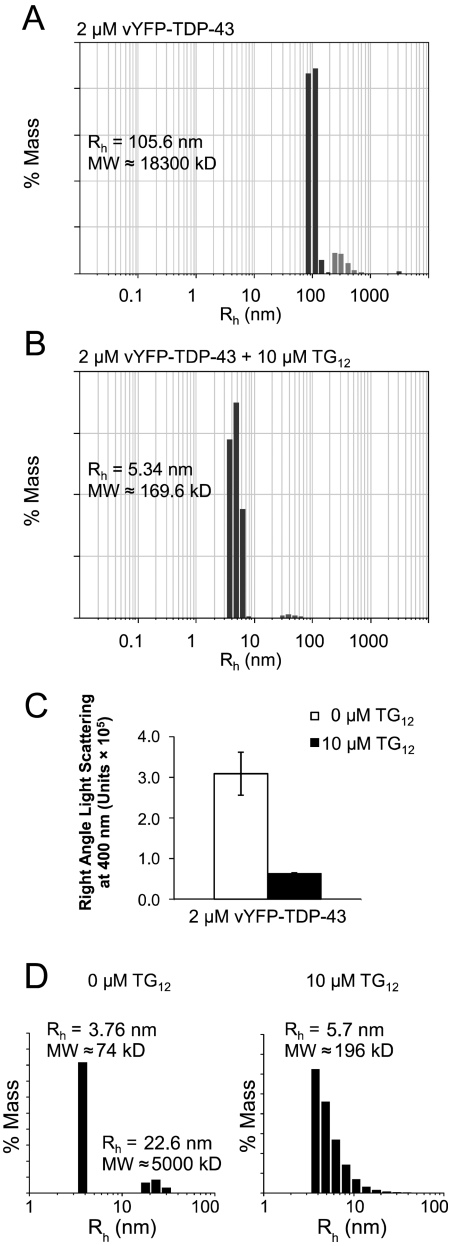

Figure 2. Size distribution by mass of vYFP-TDP-43 upon aggregation determined by dynamic light scattering and sample turbidity measured by right angle light scattering. (A) vYFP-TDP-43 (2 μM) was placed under aggregation conditions for 4 h at 20 °C. (B) The same conditions were applied to the sample in the presence of 10 μM TG_{12}. Measurements of Rh and MW were taken using appropriate software (see Experimental Procedures). (C) Turbidities of samples under conditions A and B were measured using right angle light scattering at 400 nm. (D) DLS of the soluble fraction of samples under conditions A and B. Identified peak sizes are indicated.

aggregation under these experimental conditions, and that inhibition of aggregation occurs by preservation of the protein's native dimeric state and prevention of a monomeric state.

To quantify the potency of aggregation inhibition, a concentration dependency assay was conducted using TG_{12} ssDNA monitored by RALS. Under the same conditions that were used for the DLS assays, vYFP-TDP-43 was induced to aggregate in the presence of varying concentrations of TG_{12} ssDNA (0−2 μM) and AC_{12} ssDNA as a negative control (0−10 μM) (Figure 3). A concentration dependence of inhibition

dx.doi.org/10.1021/bi500617x | Biochemistry 2014, 53, 5885−5894

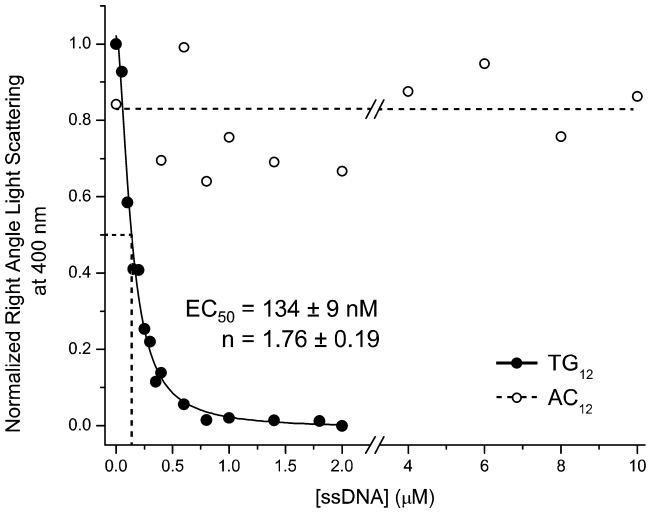

Figure 3. Inhibition of vYFP-TDP-43 aggregation using TG_{12} monitored by right angle light scattering. vYFP-TDP-43 (2 μM) was incubated with varying concentrations of TG_{12} (●) and AC_{12} (○) ssDNA under aggregation conditions for 4 h. Turbidity was determined by right angle light scattering at 400 nm. The inhibition curve of TG_{12} was fit by nonlinear least-squares fitting using eq 1, and the EC_{50} and n values are listed.

was observed with the TG_{12} ssDNA, and the data were fit using nonlinear least-squares fitting to eq 1. An effective concentration (EC_{50}) of 134 nM TG_{12} was observed for the aggregation inhibition of a sample containing 2 μM vYFP-TDP-43 (n = 1.75). The maximal effect of inhibition appears to have been achieved at 1 μM TG_{12}, a substoichiometric 1:2 molar ratio of compound and recombinant protein. For samples treated with AC_{12}, no effect was observed even at a 5-fold molar excess of oligonucleotide.

Naturally Occurring Nucleotide Targets Reduce the Level of TDP-43 Aggregation. Although TG_{12} repeats show strong binding to vYFP-TDP-43, the majority of targets of TDP-43 identified by UV cross-linking immunoprecipitation (UV-CLIP) assays do not have long stretches of consecutive poly-TG and poly-UG residues.[33,34] To assess whether oligonucleotides already present in the cell are capable of inhibiting TDP-43 aggregation, biologically relevant targets of TDP-43 are examined as potential aggregation inhibitors. The first target we selected is the transactive response (TAR) element of human immunodeficiency virus-1 (HIV1), the first binding target of TDP-43 through which the protein was discovered.[24] TDP-43 binds to a sequence on the viral element on the long terminal repeat (LTR) sequence of the integrated viral genome, responsible for the TAR element. Although not normally found in healthy cells, this binding sequence holds historical significance and also contains two pyrimidine regions, which are consensus sequences for TDP-43 binding.[33] TDP-43 not only was found to bind the double-stranded TAR cDNA but also has minor affinity for the coding single-strand sequence.[24] We decided to assess the effect of both double-stranded and single-stranded HIV1 LTR on TDP-43 aggregation. Another sequence we selected is a stretch of a guanine-rich sequence located at the 3′UTR of TDP-43 mRNA discovered by UV-CLIP, denoted by CLIP34nt.[35] We chose this sequence as a candidate RNA sequence for inhibiting TDP-43 aggregation because it is involved in TDP-43 autoregulation. The potential of TDP-43's autoregulation to be linked to its solubility can be of particular interest with respect to its role in disease.

Using TG_{12} and AC_{12} as positive and negative controls, respectively, the aggregation inhibition of vYFP-TDP-43 by CLIP34nt RNA, HIV1LTR ssDNA, and HIV1LTR dsDNA was examined using RALS using methods and conditions described above (Figure 4A). Calculated EC_{50} and n values (Figure 4B) for CLIP34nt RNA and HIV1LTR ssDNA are approximately 2 μM and ~0.5, respectively. Although the potency of inhibition is weaker than that of the TG_{12} control (205 nM), they demonstrate that binding of natural ligands of TDP-43 has an inhibitory effect on the aggregation of this protein. The HIV1LTR dsDNA did not have an effect on the aggregation of vYFP-TDP-43 despite its reported ability to bind to this protein determined by previous studies.[24]

Aggregation Inhibition Is Achieved through RRM1 Binding. Previous studies have demonstrated that TG_{12} fails to inhibit TDP-43 aggregation in the absence of a functional RRM1 domain, where phenylalanine residues critical for DNA/RNA binding are mutated (F147L and F149L mutations).[22] Truncations of RRM1 also demonstrated the same effect. Additionally, F147L and F149L mutations also disrupted TDP-43 autoregulation.[25] We thus suspect aggregation inhibition using naturally occurring compounds is also mediated through binding to RRM1. When the right angle light scattering experiments are repeated on DNA/RNA binding-deficient mutants of TDP-43, we observe no change in scattering upon addition of TG_{12} or CLIP34nt oligonucleotides (Figure 4C) compared to that of the wild-type (wt) protein control. This confirms that aggregation inhibition is accomplished through the binding interaction between a specific oligonucleotide target and the RRM1 domain of TDP-43.

Irreversible Nature of vYFP-TDP-43 Aggregation. Our data suggest that by binding to the native, dimeric state of vYFP-TDP-43, native-state binding molecules can prevent the protein from entering the aggregation pathway. The following experiments assess whether these compounds have disaggregation properties once the protein has already entered the aggregated state. These results serve a secondary purpose of providing visual validation to the observations in RALS measurements. Samples were observed under a fluorescence microscope after incubation for 20 min under aggregating conditions in the presence or absence of aggregation-inhibiting nucleotides. By visual inspection, samples induced to aggregate in the presence of TG_{12} showed largely diffuse distributions, with few small particulates (Figure 5). Untreated samples and those treated with AC_{12} exhibited large aggregates up to 100 μm in diameter. This result is in accordance with the RALS assays previously performed. When samples were subjected to aggregation for 15 min, followed by addition of various ssDNA molecules for an additional 5 min, no changes in aggregation were observed (Figure 5). These samples remain unchanged after 24 h, and all samples contained aggregates with a similar morphology. These results indicate that although native-state binding molecules can reduce the propensity for entry into the aggregated state, preformed aggregates cannot be dissolved by the addition of these compounds and the aggregation process is irreversible.

Morphology of TDP-43 Aggregates. Solutions of vYFP-TDP-43 incubated for 20 min at room temperature under aggregating conditions were imaged using AFM with a glass tapping fluid cell to assess the overall aggregate morphology on a mica surface. The resulting images show formations of small

dx.doi.org/10.1021/bi500617x | Biochemistry 2014, 53, 5885−5894

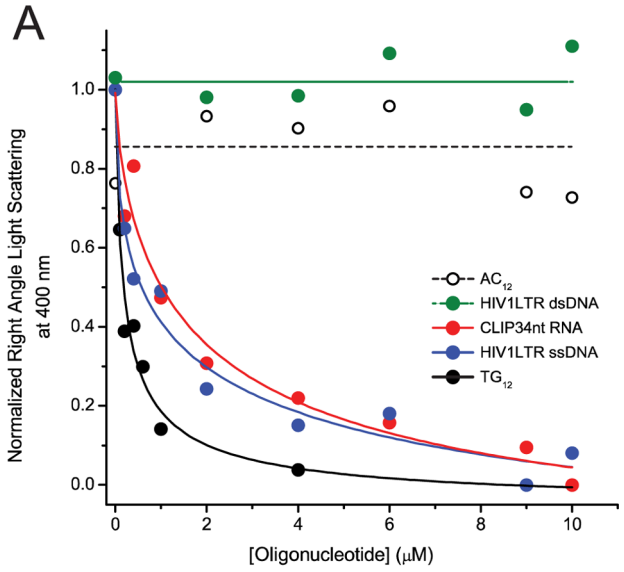

B

Calculated EC_{50} Values

Oligonucleotide	EC_{50} (nM)	n
AC_{12}	N/A	N/A
HIV1LTR dsDNA	N/A	N/A
HIV1LTR ssDNA	1856 ± 3797	0.48 ± 0.24
CLIP34nt	1874 ± 2186	0.69 ± 0.31
TG_{12}	205 ± 67	0.76 ± 0.26
AC_{12}	5′ACACACACACACACACACACAC 3′	
HIV1LTR	5′TGCTTTTTGCCTGTACTGGGTCTCTCTGGTTAGACCAGATCTGAG 3′	
CLIP34nt	5′GAGAGAGCGCGUGCAGAGACUUGGUGGUGCAUAA 3′	
TG_{12}	5′TGTGTGTGTGTGTGTGTGTGTG 3′	

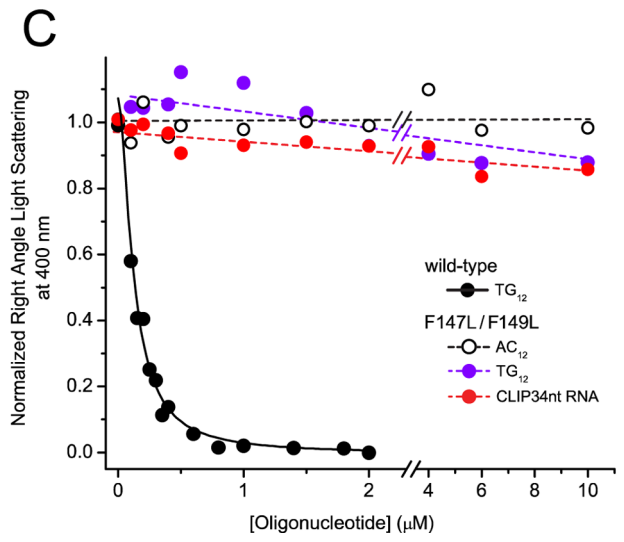

Figure 4. Inhibition of wild-type (wt) and F147L/F149L mutant vYFP-TDP-43 aggregation using various natural oligonucleotide binding targets. (A) Protein (2 μM) was incubated under aggregating conditions with varying concentrations of different nucleotides for 4 h. Turbidity was determined by right angle light scattering at 400 nm. (B) Calculated EC_{50} values, names, and sequences of nucleotides used for native-state stabilization. EC_{50} and n values were obtained by nonlinear least-squares fitting using eq 1. (C) Aggregation assays were performed on 2 μM F147L/F149L mutant protein using TG_{12}, AC_{12}, and CLIP34nt and results compared to those for wt protein treated with TG_{12} as a control.

Figure 4. continued

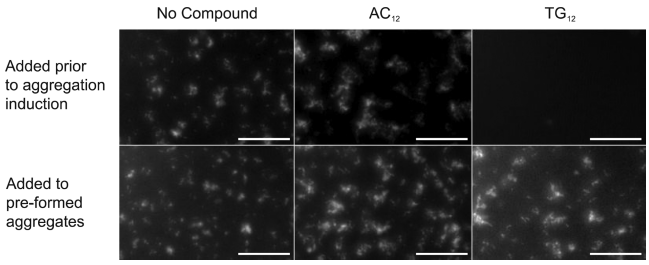

Figure 5. Fluorescence microscopy of vYFP-TDP-43 aggregates. Images were taken at 20 °C targeting the vYFP tag (λ_{ex} = 515 nm; λ_{em} = 528) using a 10× objective and a 40× lens. vYFP-TDP-43 (2 μM) was incubated for 20 min under aggregating conditions in the presence of various ssDNAs (bottom row). Various ssDNAs were added to preformed aggregates upon incubation for 15 min, and images were taken 5 min after the addition of ssDNA (bottom row). The scale bar represents 100 μm.

clusters of globular structures ranging from 10 to 100 nm in diameter (Figure 6). The aggregates are nonfibrillar and show no apparent order.

DISCUSSION

TDP-43 aggregation has been implicated as a key step in ALS and FTD pathogenesis, but the mechanism of aggregation remains enigmatic. Several factors have been proposed to influence TDP-43 aggregation, including oxidative stress, heat shock, stress granule formation, cleavage into C-terminal fragments, and loss of DNA/RNA targets.[20,21,36−40] Binding of TDP-43 to the artificial sequence of poly-TG repeats improves its solubility, and C-terminal fragments of TDP-43 containing RRM2 and C-terminal domains remain soluble in cell culture unless they are treated with RNase I.[21,22] TDP-43, as an intrinsically aggregation-prone protein, remains soluble in the nucleus even when it is overexpressed in cell culture.[22,28] This suggests a crucial role of RNA in TDP-43 solubility. Our findings support the hypothesis that TDP-43 undergoes a conformational change from its native state to an aggregation-prone state triggered by the loss of its native binding partners, priming it for environmental factors that may lead to its aggregation.

Insights into TDP-43 Misfolding and Inhibition Mechanisms. Our findings confirm previous work on TDP-43 aggregation attenuation through TG_{12} binding.[22] In our studies, we measured aggregation using DLS and RALS with recombinant vYFP-TDP-43 that is natively β-structured, folded, and dimeric. Via comparison of the size distribution of aggregates upon induction in the presence and absence of a 5-fold molar excess of TG_{12}, it is apparent that in the absence of TG_{12}, vYFP-TDP-43 formed large oligomeric species hundreds of nanometers in size (Figure 2B). When the sample was treated with TG_{12}, 95% of the sample remained dimeric (Figure 2A), suggesting that the presence of TG_{12} was able to prevent vYFP-TDP-43 from entering any downstream aggregation-prone pathways. In many cases of protein misfolding such as transthyretin (TTR) and superoxide dismutase 1 (SOD1), the primary step in the misfolding pathway usually involves dissociation of the native oligomer into an aggregation-prone

dx.doi.org/10.1021/bi500617x | Biochemistry 2014, 53, 5885−5894

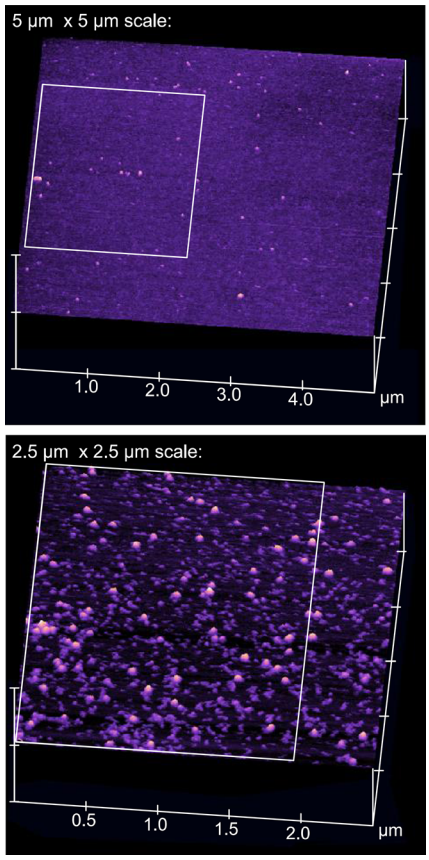

Figure 6. Tapping mode atomic force microscopy images of nonfibrillar vYFP-TDP-43 aggregates. Images were acquired in a solution consisting of 2 μM vYFP-TDP-43, 170 mM KCl, 36 mM HEPES, 25 mM imidazole, 18 mM $MgCl_2$, 1% glycerol, and 1.8 mM βME (pH 7.4) by tapping mode AFM after deposition onto a mica surface. Two image sizes are provided: 5 μm × 5 μm (top) and 2.5 μm × 2.5 μm (bottom), on a 0.5−5 μm height scale. Boxes in both panels indicate the same imaged region using different scales. The bottom panel is shown with an increased contrast, and the height scale is the same in both panels.

monomer.[41−43] We have found evidence to suggest that this is also a likely mechanism of TDP-43 aggregation observed under our experimental conditions because of the presence of monomeric and soluble oligomeric TDP-43 in the soluble fraction of samples under aggregating conditions (Figure 2D and Figure S1C of the Supporting Information). Our data suggest that maintenance of the native dimer through DNA binding prevents the downstream aggregation processes, which likely involves an initial monomerization event. We observed the same inhibitory effect using RALS and fluorescence microscopy assays, consistent with our initial findings (Figures 2C and 5). The fluorescence assay also showed that preformed aggregates could not be rescued by the presence of the TG_{12} compound, consistent with the idea that the aggregation pathway leads to an irreversible end product, which is a common hallmark of non-native aggregation of proteins detailed in various reviews.[44,45] Morphologically, we found that the aggregates, like those observed in ALS neurons, did not share the characteristic fibrillar structure of prion aggregates (Figure 6).[4,46] However, because of the absence of structural data for TDP-43's C-terminus under native or aggregating conditions, we cannot confirm that the aggregates observed in our *in vitro* assays are identical in morphology or behavior to those in disease neurons. Whether oligonucleotides can reverse aggregates in *in vivo* systems remains to be tested. We generated an inhibition curve by altering the TG_{12} concentration while measuring turbidity using RALS and calculated the EC_{50} value of this inhibition as 134 nM with a Hill coefficient of 1.75 (Figure 3). A coefficient of >1 in the context of EC_{50} measurements suggests multiple binding sites.[47] This is expected, as a single TG_{12} molecule should be able to bind at least two TDP-43 molecules, potentially serving as a tether to stabilize the native dimer. In fact, we observed that a 1:2 TG_{12}:protein molar ratio was sufficient to achieve maximal inhibition, while AC_{12} had no effect. This substoichiometric effect specific to a binding partner in conjunction with the presence of exclusively dimeric species in our DLS results suggests that TG_{12} inhibits vYFP-TDP-43 aggregation by binding to the native dimer, acting as a chaperone to prevent aggregation initiation. Furthermore, F147L and F149L mutations on RRM1 abolish this inhibition effect, confirming that the specificity of oligonucleotide targets is achieved through a functional RRM1 domain (Figure 4C). There is a general consensus that the C-terminus of TDP-43 is a key player in this aggregation pathway.[12,14] It is a GQN-rich prion-like domain and has been shown to have prion-like properties.[11,12,16] Specifically, expression of 12 tandem repeats of residues 331−369 of the C-terminus containing Q/N-rich sequences is sufficient to form aggregates in which native nuclear TDP-43 can be sequestered.[12] Seeding of C-terminal fragments from diseased brains into the cell culture can also recapitulate disease phenotypes.[16] However, this proposed intrinsically disordered C-terminal region is not required for oligonucleotide interactions,[10] yet we find that native-state binding molecules effectively reduce the level of aggregation caused by this C-terminal region without physical interactions. This suggests that there are likely structural differences with the C-terminal region of TDP-43 when the protein is a native dimer versus a non-native, aggregation-prone monomer, and that the retention of TDP-43 in its native state by the binding of native-state binding compounds prevents the C-terminus from engaging in aggregation-prone interactions with C-termini of non-native TDP-43 *in vitro*. Recent studies show that the C-terminus is intrinsically disordered, but Q/N-rich segments (residues 341−366) are able to spontaneously form β-rich species, through which aggregation may arise.[48] Co-immunoprecipitation experiments using FLAG-TDP-43 in cells show that FLAG-TDP-43 coprecipitates with full length TDP-43, suggesting TDP-43 self-interactions. The coprecipitation efficiency was reduced drastically when the process was conducted on cells expressing TDP-43 with deletion of the C-terminus.[49] This suggests that the C-terminus has a role in maintaining TDP-43 as a dimer in the native state, which is affected by cognate DNA/RNA binding. Factors that disrupt these properties of TDP-43, including ALS-causing mutations on the C-terminus or loss of cognate DNA/RNA partners (through mislocalization, cleavage, or RNA binding-deficient mutations), may make TPD-43 more likely to adopt an aggregation-prone conformation on the C-terminus, increasing its propensity to aggregate.

Implications of TDP-43 Aggregation Inhibition by Naturally Occurring Targets. TDP-43 has a variety of cellular roles, and the C-terminus has been implicated in many protein−protein interactions such as binding to heterogeneous nuclear ribonucleoproteins (hnRNPs) to participate in mRNA splicing, degradation, stabilization, and other various func-

dx.doi.org/10.1021/bi500617x | *Biochemistry* 2014, 53, 5885−5894

tions.[13,19] In cells where these protein−protein interactions are prevalent, many factors likely contribute to TDP-43 solubility. From our findings, cognate binding to its mRNA targets appears to be an additional factor for maintaining TDP-43 solubility under normal conditions. This aggregation inhibitory effect was observed for single-stranded DNA and RNA, but not the double-stranded DNA target. We propose that the majority of TDP-43 in the nucleus is bound to a DNA/RNA target, which maintains its solubility in healthy cells. One of the binding partners readily available to newly synthesized TDP-43 is the 3′UTR of its own mRNA. TDP-43 levels in cells are regulated through a negative feedback loop in which TDP-43 binds to the 3′UTR of its own mRNA promoting mRNA instability.[25,50] We find that binding of CLIP34nt to TDP-43 through RRM1 increases TDP-43 solubility (Figure 4). Binding of TDP-43 to its own mRNA may have a 2-fold effect: it may increase the solubility of the newly synthesized protein while simultaneously targeting the mRNA for degradation. Such a finding suggests additional layers of complexity in the spatiotemporal regulation of TDP-43 that previously may not have been considered. Similar mechanisms of native-state stabilization via DNA binding to a tightly regulated protein have also been observed in tumor suppressor p53, where a consensus DNA sequence binding to p53's core domain (p53C) can stabilize the full length protein and prevent amyloid-like aggregation.[51]

Disruption of interactions between TDP-43 and its own mRNA may promote newly synthesized TDP-43 to adopt a β-rich aggregation-prone fold at its C-terminus, while simultaneously increasing TDP-43 levels due to disruption of the autoregulation pathway, leading to increased concentrations of aggregation-prone TDP-43 species in the cell and making it vulnerable to environmental factors. This serves as the first "hit" in a "two-hit" hypothesis proposed by Persiridis and colleagues.[21] Cellular stresses such as oxidative damage and heat shock in the presence of the larger population of aggregation-prone species provide the second hit, leading to the potential recruitment of these proteins into SG, creating irreversible aggregates and inclusion bodies as seen in ALS neurons. Whereas the C-terminus of TDP-43 normally allows for transient and reversible interactions in SG under non-pathological conditions, other factors proposed to affect TDP-43 aggregation such as C-terminal phosphorylation and cytoplasmic localization may also serve as initial steps to expose the protein to vulnerability by increasing the propensity of the C-terminus to adopt an aggregation-prone fold and effectively reduce the number of locally available native binding partners, respectively. The loss of functional TDP-43 through misregulation and an increased number of aggregates in the cell may cause ALS-related pathology through both loss of TDP-43 function and gain of TDP-43 aggregate toxic function mechanisms. It is uncertain which mechanism is predominant in disease. Recent studies of TDP-43 mutants such as F147L/F149L in a number of model organisms show that the expression of exogenous wt TDP-43 can generate more neurotoxicity than expression of mutant TDP-43.[52,53] We believe that in the context of *in vivo* systems, introduction of exogenous TDP-43 may be disruptive to the RNA binding activities of the endogenous protein. Because of its myriad of roles in RNA processing, exogenous TDP-43 expression may replicate the effect of disrupted TDP-43 autoregulation. The inability of the F147L/F149L mutant to generate toxicity while still forming aggregates in these system may suggest that depletion of native TDP-43 function (through mutations or aggregation) is the key factor in generating neurotoxicity and may not always be dependent on aggregation.[53]

The need for neurons to spatially and temporally regulate their transcription dictates the movement of mRNA/RNA binding protein complexes across long neuronal processes. The long turnover time for these proteins and complexes may render these proteins more susceptible to oxidative damage or other environmental stressors, which may explain why disease phenotypes are specific to neurons and no other cell types. Recently, many RNA binding proteins with intrinsically disordered regions such as Fused in Sarcoma/Translocated in Sarcoma (FUS/TLS) have also been implicated in neurodegenerative diseases and formation of SG, which may cause pathology via a mechanism similar to that of TDP-43.[54−56]

Herein we determined that TDP-43 mRNA's 3′UTR can bind TDP-43 as a native-state stabilizer and as a potential intrinsic folding chaperone for newly synthesized protein and propose a potential pathway through which TDP-43 aggregation and neurotoxicity may occur.

■ ASSOCIATED CONTENT

Supporting Information

A figure containing visual representations of the wt and F147L/F149L mutant vYFP-TDP-43 constructs, primer sequences used to produce the mutant, and an annotated graphical representation of the proposed aggregation pathway. This material is available free of charge via the Internet at http://pubs.acs.org.

■ AUTHOR INFORMATION

Corresponding Author

*University Health Network, Toronto Medical Discovery Tower, MaRS Centre, 101 College St., Room 4-305, Toronto, Ontario M5G 1L7, Canada. E-mail: chakrab@uhnres.utoronto.ca. Phone and fax: (416) 581-7554.

Funding

Supported by the Alzheimer's Society of Canada and the Ontario Government.

Notes

The authors declare no competing financial interest.

■ ACKNOWLEDGMENTS

The vector containing human TDP-43 sequence was a kind gift from Dr. Janice Robertson. We thank Dr. Douglas V. Laurents, Dr. Fracisco Baralle, and Dr. Emanuele Buratti for their constructive comments and insightful discussions.

■ ABBREVIATIONS

TDP-43, TAR DNA binding protein of 43 kDa; TAR, transactive response; ALS, amyotrophic lateral sclerosis; RRM, RNA recognition motif; SG, stress granules; TTR, transthyretin; DLS, dynamic light scattering; HIV1, human immunodeficiency virus-1; LTR, long terminal repeat; RALS, right angle light scattering; SOD1, superoxide dismutase 1; NMD, nonsense-mediated decay; UV-CLIP, UV cross-linking immunoprecipitation; FUS/TLS, Fused in Sarcoma/Translocated in Sarcoma.

■ REFERENCES

(1) Schenk, D., Barbour, R., Dunn, W., Gordon, G., Grajeda, H., Guido, T., Hu, K., Huang, J., Johnson-Wood, K., Khan, K.,

Kholodenko, D., Lee, M., Liao, Z., Lieberburg, I., Motter, R., Mutter, L., Soriano, F., Shopp, G., Vasquez, N., Vandevert, C., Walker, S., Wogulis, M., Yednock, T., Games, D., and Seubert, P. (1999) Immunization with amyloid-β attenuates Alzheimer-disease-like pathology in the PDAPP mouse. *Nature 400*, 173−177.
(2) Polymeropoulos, M. H. (1997) Mutation in the α-Synuclein Gene Identified in Families with Parkinson's Disease. *Science 276*, 2045−2047.
(3) Majoor-Krakauer, D., Willems, P. J., and Hofman, A. (2003) Genetic epidemiology of amyotrophic lateral sclerosis. *Clin. Genet. 63*, 83−101.
(4) Neumann, M., Sampathu, D. M., Kwong, L. K., Truax, A. C., Micsenyi, M. C., Chou, T. T., Bruce, J., Schuck, T., Grossman, M., Clark, C. M., McCluskey, L. F., Miller, B. L., Masliah, E., Mackenzie, I. R., Feldman, H., Feiden, W., Kretzschmar, H. A., Trojanowski, J. Q., and Lee, V. M.-Y. (2006) Ubiquitinated TDP-43 in frontotemporal lobar degeneration and amyotrophic lateral sclerosis. *Science 314*, 130−133.
(5) Arai, T., Hasegawa, M., Akiyama, H., Ikeda, K., Nonaka, T., Mori, H., Mann, D., Tsuchiya, K., Yoshida, M., Hashizume, Y., and Oda, T. (2006) TDP-43 is a component of ubiquitin-positive tau-negative inclusions in frontotemporal lobar degeneration and amyotrophic lateral sclerosis. *Biochem. Biophys. Res. Commun. 351*, 602−611.
(6) Kabashi, E., Valdmanis, P. N., Dion, P., Spiegelman, D., McConkey, B. J., Vande Velde, C., Bouchard, J.-P., Lacomblez, L., Pochigaeva, K., Salachas, F., Pradat, P.-F., Camu, W., Meininger, V., Dupre, N., and Rouleau, G. A. (2008) TARDBP mutations in individuals with sporadic and familial amyotrophic lateral sclerosis. *Nat. Genet. 40*, 572−574.
(7) Lagier-Tourenne, C., Polymenidou, M., and Cleveland, D. W. (2010) TDP-43 and FUS/TLS: Emerging roles in RNA processing and neurodegeneration. *Hum. Mol. Genet. 19*, R46−R64.
(8) Buratti, E., and Baralle, F. E. (2001) Characterization and functional implications of the RNA binding properties of nuclear factor TDP-43, a novel splicing regulator of CFTR exon 9. *J. Biol. Chem. 276*, 36337−36343.
(9) Buratti, E., Brindisi, A., Pagani, F., and Baralle, F. E. (2004) Nuclear factor TDP-43 binds to the polymorphic TG repeats in CFTR intron 8 and causes skipping of exon 9: A functional link with disease penetrance. *Am. J. Hum. Genet. 74*, 1322−1325.
(10) Kuo, P.-H., Doudeva, L. G., Wang, Y.-T., Shen, C.-K. J., and Yuan, H. S. (2009) Structural insights into TDP-43 in nucleic-acid binding and domain interactions. *Nucleic Acids Res. 37*, 1799−1808.
(11) Gitler, A. D., and Shorter, J. (2011) RNA-binding proteins with prion-like domains in ALS and FTLD-U. *Prion 5*, 179−187.
(12) Budini, M., Buratti, E., Stuani, C., Guarnaccia, C., Romano, V., De Conti, L., and Baralle, F. E. (2012) Cellular model of TAR DNA-binding protein 43 (TDP-43) aggregation based on its C-terminal Gln/Asn-rich region. *J. Biol. Chem. 287*, 7512−7525.
(13) Buratti, E., Brindisi, A., Giombi, M., Tisminetzky, S., Ayala, Y. M., and Baralle, F. E. (2005) TDP-43 binds heterogeneous nuclear ribonucleoprotein A/B through its C-terminal tail: An important region for the inhibition of cystic fibrosis transmembrane conductance regulator exon 9 splicing. *J. Biol. Chem. 280*, 37572−37584.
(14) Igaz, L. M., Kwong, L. K., Chen-Plotkin, A., Winton, M. J., Unger, T. L., Xu, Y., Neumann, M., Trojanowski, J. Q., and Lee, V. M.-Y. (2009) Expression of TDP-43 C-terminal Fragments in Vitro Recapitulates Pathological Features of TDP-43 Proteinopathies. *J. Biol. Chem. 284*, 8516−8524.
(15) Zhang, Y.-J., Xu, Y.-F., Cook, C., Gendron, T. F., Roettges, P., Link, C. D., Lin, W.-L., Tong, J., Castanedes-Casey, M., Ash, P., Gass, J., Rangachari, V., Buratti, E., Baralle, F., Golde, T. E., Dickson, D. W., and Petrucelli, L. (2009) Aberrant cleavage of TDP-43 enhances aggregation and cellular toxicity. *Proc. Natl. Acad. Sci. U.S.A. 106*, 7607−7612.
(16) Nonaka, T., Masuda-Suzukake, M., Arai, T., Hasegawa, Y., Akatsu, H., Obi, T., Yoshida, M., Murayama, S., Mann, D. M. A., Akiyama, H., and Hasegawa, M. (2013) Prion-like properties of pathological TDP-43 aggregates from diseased brains. *Cell Rep. 4*, 124−134.
(17) Barmada, S. J., Skibinski, G., Korb, E., Rao, E. J., Wu, J. Y., and Finkbeiner, S. (2010) Cytoplasmic mislocalization of TDP-43 is toxic to neurons and enhanced by a mutation associated with familial amyotrophic lateral sclerosis. *J. Neurosci. 30*, 639−649.
(18) Giordana, M. T., Piccinini, M., Grifoni, S., De Marco, G., Vercellino, M., Magistrello, M., Pellerino, A., Buccinnà, B., Lupino, E., and Rinaudo, M. T. (2010) TDP-43 redistribution is an early event in sporadic amyotrophic lateral sclerosis. *Brain Pathol. 20*, 351−360.
(19) McDonald, K. K., Aulas, A., Destroismaisons, L., Pickles, S., Beleac, E., Camu, W., Rouleau, G. A., and Vande Velde, C. (2011) TAR DNA-binding protein 43 (TDP-43) regulates stress granule dynamics via differential regulation of G3BP and TIA-1. *Hum. Mol. Genet. 20*, 1400−1410.
(20) Parker, S. J., Meyerowitz, J., James, J. L., Liddell, J. R., Crouch, P. J., Kanninen, K. M., and White, A. R. (2012) Endogenous TDP-43 localized to stress granules can subsequently form protein aggregates. *Neurochem. Int. 60*, 415−424.
(21) Pesiridis, G. S., Tripathy, K., Tanik, S., Trojanowski, J. Q., and Lee, V. M.-Y. (2011) A "two-hit" hypothesis for inclusion formation by carboxyl-terminal fragments of TDP-43 protein linked to RNA depletion and impaired microtubule-dependent transport. *J. Biol. Chem. 286*, 18845−18855.
(22) Huang, Y.-C., Lin, K.-F., He, R.-Y., Tu, P.-H., Koubek, J., Hsu, Y.-C., and Huang, J. J.-T. (2013) Inhibition of TDP-43 Aggregation by Nucleic Acid Binding. *PLoS One 8*, e64002.
(23) Ayala, Y. M., Pantano, S., D'Ambrogio, A., Buratti, E., Brindisi, A., Marchetti, C., Romano, M., and Baralle, F. E. (2005) Human, *Drosophila*, and *C. elegans* TDP43: Nucleic acid binding properties and splicing regulatory function. *J. Mol. Biol. 348*, 575−588.
(24) Ou, S. H., Wu, F., Harrich, D., García-Martínez, L. F., and Gaynor, R. B. (1995) Cloning and characterization of a novel cellular protein, TDP-43, that binds to human immunodeficiency virus type 1 TAR DNA sequence motifs. *J. Virol. 69*, 3584−3596.
(25) Ayala, Y. M., De Conti, L., Avendaño-Vázquez, S. E., Dhir, A., Romano, M., D'Ambrogio, A., Tollervey, J., Ule, J., Baralle, M., Buratti, E., and Baralle, F. E. (2011) TDP-43 regulates its mRNA levels through a negative feedback loop. *EMBO J. 30*, 277−288.
(26) Budini, M., and Buratti, E. (2011) TDP-43 autoregulation: Implications for disease. *J. Mol. Neurosci. 45*, 473−479.
(27) Bembich, S., Herzog, J. S., De Conti, L., Stuani, C., Avendaño-Vázquez, S. E., Buratti, E., Baralle, M., and Baralle, F. E. (2014) Predominance of spliceosomal complex formation over polyadenylation site selection in TDP-43 autoregulation. *Nucleic Acids Res. 42*, 3362−3371.
(28) Johnson, B. S., Snead, D., Lee, J. J., McCaffery, J. M., Shorter, J., and Gitler, A. D. (2009) TDP-43 is intrinsically aggregation-prone, and amyotrophic lateral sclerosis-linked mutations accelerate aggregation and increase toxicity. *J. Biol. Chem. 284*, 20329−20339.
(29) Nagai, T., Ibata, K., Park, E. S., Kubota, M., Mikoshiba, K., and Miyawaki, A. (2002) A variant of yellow fluorescent protein with fast and efficient maturation for cell-biological applications. *Nat. Biotechnol. 20*, 87−90.
(30) Arslan, P. E., and Chakrabartty, A. (2009) Probing Alzheimer amyloid peptide aggregation using a cell-free fluorescent protein refolding method. *Biochem. Cell Biol. 87*, 631−639.
(31) Greenfield, N. J. (2006) Using circular dichroism spectra to estimate protein secondary structure. *Nat. Protoc. 1*, 2876−2890.
(32) Rekas, A., Alattia, J.-R., Nagai, T., Miyawaki, A., and Ikura, M. (2002) Crystal structure of Venus, a yellow fluorescent protein with improved maturation and reduced environmental sensitivity. *J. Biol. Chem. 277*, 50573−50578.
(33) Xiao, S., Sanelli, T., Dib, S., Sheps, D., Findlater, J., Bilbao, J., Keith, J., Zinman, L., Rogaeva, E., and Robertson, J. (2011) RNA targets of TDP-43 identified by UV-CLIP are deregulated in ALS. *Mol. Cell. Neurosci. 47*, 167−180.
(34) Tollervey, J. R. J., Curk, T., Rogelj, B., Briese, M., Cereda, M., and Ule, J. (2011) Characterising the RNA targets and position-

dependent splicing regulation by TDP-43; implications for neurodegenerative diseases. *Nat. Neurosci. 14*, 452−458.
(35) Bhardwaj, A., Myers, M. P., Buratti, E., and Baralle, F. E. (2013) Characterizing TDP-43 interaction with its RNA targets. *Nucleic Acids Res. 41*, 5062−5074.
(36) Zhang, T., Mullane, P. C., Periz, G., and Wang, J. (2011) TDP-43 neurotoxicity and protein aggregation modulated by heat shock factor and insulin/IGF-1 signaling. *Hum. Mol. Genet. 20*, 1952−1965.
(37) Furukawa, Y., Kaneko, K., and Nukina, N. (2011) Molecular properties of TAR DNA binding protein-43 fragments are dependent upon its cleavage site. *Biochim. Biophys. Acta 1812*, 1577−1583.
(38) Furukawa, Y., Kaneko, K., Watanabe, S., Yamanaka, K., and Nukina, N. (2011) A seeding reaction recapitulates intracellular formation of Sarkosyl-insoluble transactivation response element (TAR) DNA-binding protein-43 inclusions. *J. Biol. Chem. 286*, 18664−18672.
(39) Udan-Johns, M., Bengoechea, R., Bell, S., Shao, J., Diamond, M. I., True, H. L., Weihl, C. C., and Baloh, R. H. (2013) Prion-like nuclear aggregation of TDP-43 during heat shock is regulated by HSP40/70 chaperones. *Hum. Mol. Genet. 23*, 1−14.
(40) Liachko, N. F., Guthrie, C. R., and Kraemer, B. C. (2010) Phosphorylation promotes neurotoxicity in a *Caenorhabditis elegans* model of TDP-43 proteinopathy. *J. Neurosci. 30*, 16208−16219.
(41) Miyata, M., Sato, T., Kugimiya, M., Sho, M., Nakamura, T., Ikemizu, S., Chirifu, M., Mizuguchi, M., Nabeshima, Y., Suwa, Y., Morioka, H., Arimori, T., Suico, M. A., Shuto, T., Sako, Y., Momohara, M., Koga, T., Morino-Koga, S., Yamagata, Y., and Kai, H. (2010) The crystal structure of the green tea polyphenol (−)-epigallocatechin gallate-transthyretin complex reveals a novel binding site distinct from the thyroxine binding site. *Biochemistry 49*, 6104−6114.
(42) Mulligan, V. K., Kerman, A., Ho, S., and Chakrabartty, A. (2008) Denaturational stress induces formation of zinc-deficient monomers of Cu,Zn superoxide dismutase: Implications for pathogenesis in amyotrophic lateral sclerosis. *J. Mol. Biol. 383*, 424−436.
(43) Ip, P., Mulligan, V. K., and Chakrabartty, A. (2011) ALS-Causing SOD1 Mutations Promote Production of Copper-Deficient Misfolded Species. *J. Mol. Biol. 409*, 839−852.
(44) Morris, A. M., Watzky, M. A., and Finke, R. G. (2009) Protein aggregation kinetics, mechanism, and curve-fitting: A review of the literature. *Biochim. Biophys. Acta 1794*, 375−397.
(45) Roberts, C. (2007) Non-native protein aggregation kinetics. *Biotechnol. Bioeng. 98*, 927−938.
(46) Nonaka, T., Arai, T., Buratti, E., Baralle, F. E., Akiyama, H., and Hasegawa, M. (2009) Phosphorylated and ubiquitinated TDP-43 pathological inclusions in ALS and FTLD-U are recapitulated in SH-SY5Y cells. *FEBS Lett. 583*, 394−400.
(47) Shoichet, B. K. (2006) Interpreting steep dose-response curves in early inhibitor discovery. *J. Med. Chem. 49*, 7274−7277.
(48) Mompeán, M., Buratti, E., Guarnaccia, C., Brito, R. M. M., Chakrabartty, A., Baralle, F. E., and Laurents, D. V. (2014) Structural characterization of the minimal segment of TDP-43 competent for aggregation. *Arch. Biochem. Biophys. 545*, 53−62.
(49) Wang, I.-F., Chang, H.-Y., Hou, S.-C., Liou, G.-G., Way, T.-D., and James Shen, C.-K. (2012) The self-interaction of native TDP-43 C terminus inhibits its degradation and contributes to early proteinopathies. *Nat. Commun. 3*, 766.
(50) Polymenidou, M., and Lagier-Tourenne, C. (2011) Long pre-mRNA depletion and RNA missplicing contribute to neuronal vulnerability from loss of TDP-43. *Nat. Neurosci. 14*, 459−468.
(51) Ishimaru, D., Ano Bom, A. P. D., Lima, L. M. T. R., Quesado, P. A., Oyama, M. F. C., de Moura Gallo, C. V., Cordeiro, Y., and Silva, J. L. (2009) Cognate DNA stabilizes the tumor suppressor p53 and prevents misfolding and aggregation. *Biochemistry 48*, 6126−6135.
(52) Estes, P. S., Boehringer, A., Zwick, R., Tang, J. E., Grigsby, B., and Zarnescu, D. C. (2011) Wild-type and A315T mutant TDP-43 exert differential neurotoxicity in a *Drosophila* model of ALS. *Hum. Mol. Genet. 20*, 2308−2321.
(53) Voigt, A., Herholz, D., Fiesel, F. C., Kaur, K., Müller, D., Karsten, P., Weber, S. S., Kahle, P. J., Marquardt, T., and Schulz, J. B. (2010) TDP-43-mediated neuron loss in vivo requires RNA-binding activity. *PLoS One 5*, e12247.
(54) Baron, D. M., Kaushansky, L. J., Ward, C. L., Sama, R. R. K., Chian, R.-J., Boggio, K. J., Quaresma, A. J., Nickerson, J. A., and Bosco, D. A. (2013) Amyotrophic lateral sclerosis-linked FUS/TLS alters stress granule assembly and dynamics. *Mol. Neurodegener. 8*, 30.
(55) Deng, H.-X., Zhai, H., Bigio, E. H., Yan, J., Fecto, F., Ajroud, K., Mishra, M., Ajroud-Driss, S., Heller, S., Sufit, R., Siddique, N., Mugnaini, E., and Siddique, T. (2010) FUS-immunoreactive inclusions are a common feature in sporadic and non-SOD1 familial amyotrophic lateral sclerosis. *Ann. Neurol. 67*, 739−748.
(56) Udan, M., and Baloh, R. H. (2011) Implications of the prion-related Q/N domains in TDP-43 and FUS. *Prion 5*, 1−5.